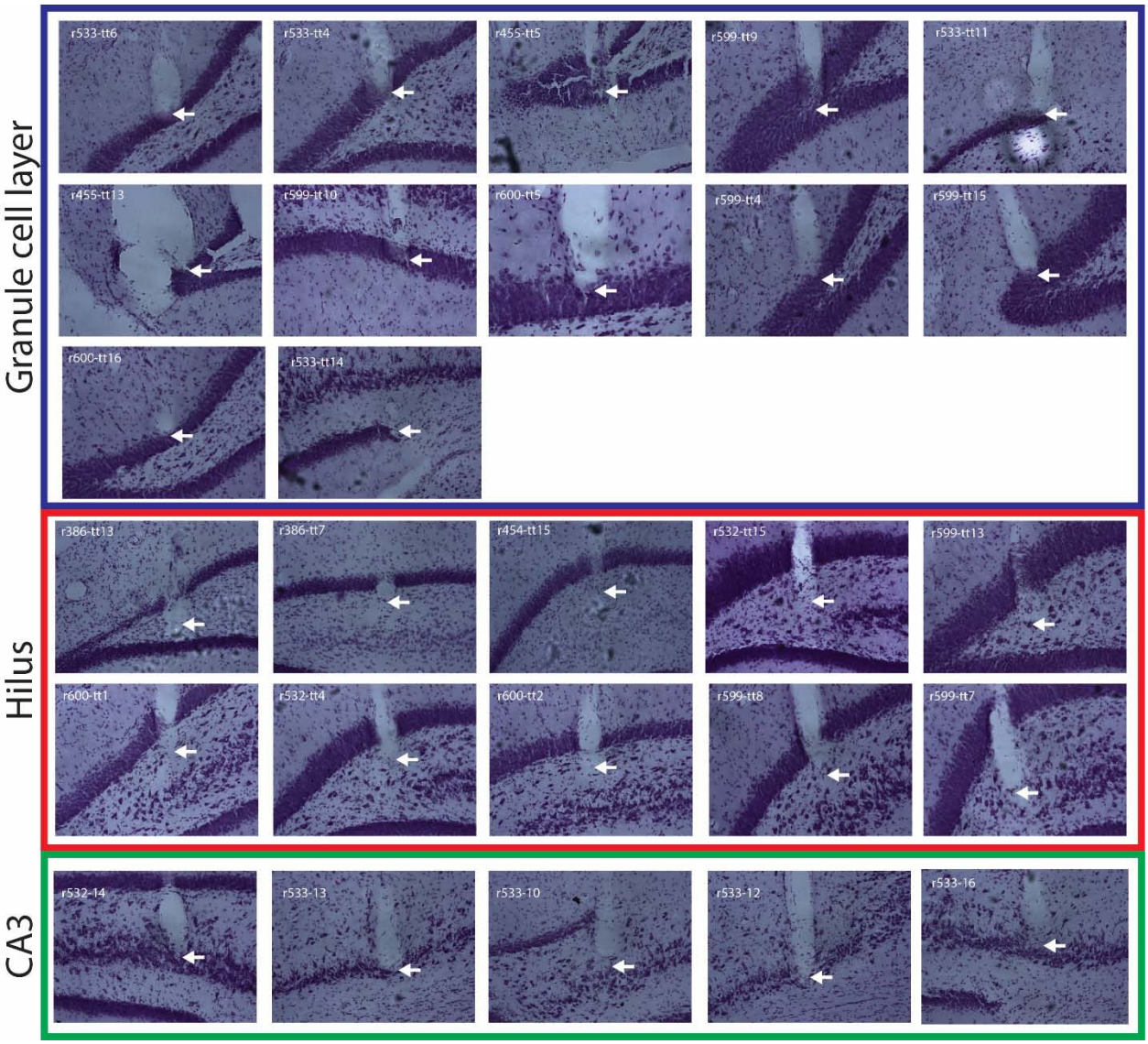

Figure S1. All tetrodes that ended clearly in the GCL, hilus, or CA3 on which cells were recorded on the final day of recording; related to Figures 1, 2

The deepest point of each tetrode track, determined by examining the brain slice under high magnification, is marked by a white arrow. All cells shown in Figure 2 and used to train the random forests classifier were recorded on the tetrodes shown here.

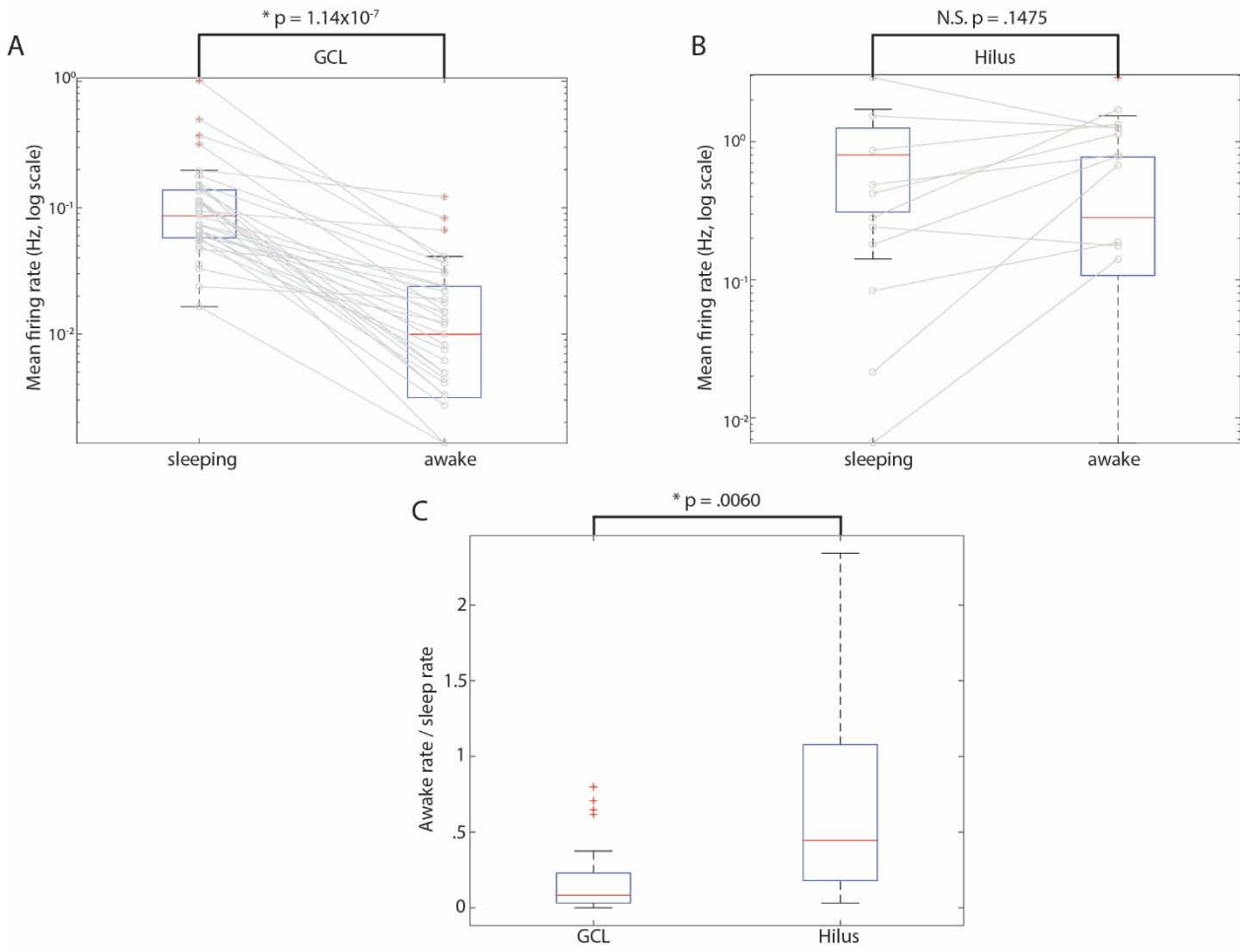

Figure S2. Mean firing rates from equal length periods of sleep and rest from 37 cells in the GCL and 11 cells in hilus; related to Figure 2

Mean firing rates of cells during sleep vs awake. Periods of sleep were defined based on a video of the sleep session. Awake periods were periods where the rat was on the pedestal during the same baseline session but not sleeping, and included time spent grooming, moving on the dish, and sitting and resting. There was no video of the baseline session for 12 hilus cells recorded on the final day, so these are not included in this plot. A, B) boxplots of the mean firing rate of cells during sleep and during an equal length period of time when the rat was awake on the pedestal. A) 37 cells recorded on the final day of recording from tetrodes histologically identified as ending in the GCL. B) 11 cells recorded on the final day of recording from tetrodes histologically identified as ending in the hilus. The firing rate of each individual cell is shown in gray. Cells in the GCL had significantly lower firing rates when the animal was awake and resting than when the animal was sleeping (Wilcoxon signed-rank test $p = 1.14x10^{-7}$). The firing rate of cells in the hilus was not significantly different in sleep and wake (Wilcoxon signed-rank test $p = 0.1475$). C) The ratio of mean rate during the awake period to the mean rate during sleep was significantly lower in the GCL than the hilus (Wilcoxon rank-sum test, $p = 0.006$), see also video S1.

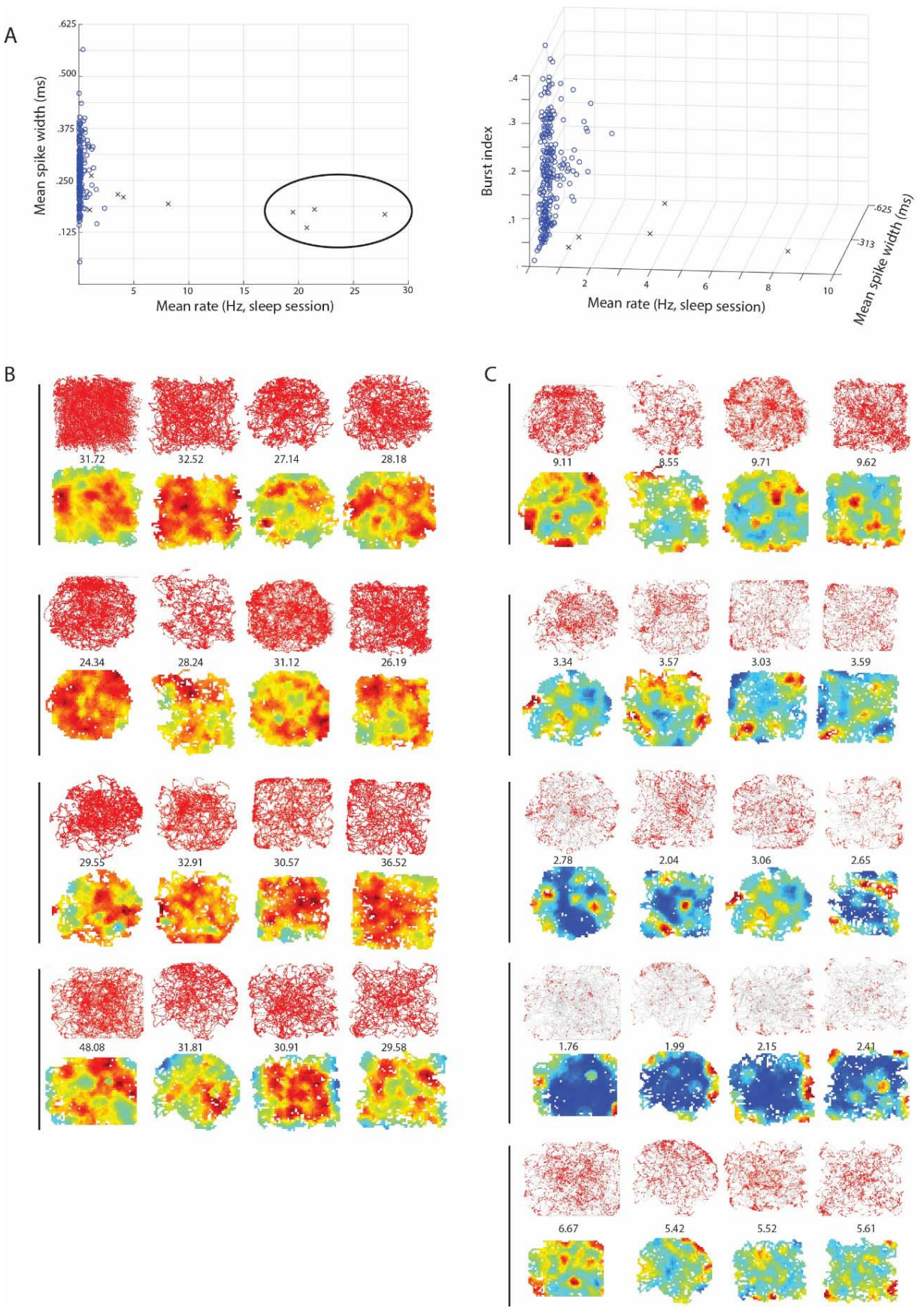
A
Mean spike width (ms)
.625
.500
.375
.250
.125
5
10
15
20
25
30
Mean rate (Hz, sleep session)
Burst index
.4
.3
.2
.1
2
4
6
8
10
Mean rate (Hz, sleep session)
.625
.313
Mean spike width (ms)
B
31.72
32.52
27.14
28.18
24.34
28.24
31.12
26.19
29.55
32.91
30.57
36.52
48.08
31.81
30.91
29.58
C
9.11
8.55
9.71
9.62
3.34
3.57
3.03
3.59
2.78
2.04
3.06
2.65
1.76
1.99
2.15
2.41
6.67
5.42
5.52
5.61

Figure S3. Putative interneurons; related to Figure 2

A) Plot of mean rate during sleep vs average spike width for each cell recorded on the final day (left) reveals a cluster of high-rate, low-width cells (circled). Consistent with previous results (Neunuebel and Knierim 2014), two additional clusters can be seen in cells with a firing rate <10 Hz. On the right, the mean firing rate, spike width and burstiness are plotted for all cells with a mean rate <10 Hz. Some cells with mean rates between 1-10 Hz and low burstiness can be separated from another group of cells with relatively low firing rates (putative excitatory neurons). In both plots blue circles represent putative excitatory neurons that were included in analysis of activity (n = 88, 37 GCL, 23 hilus, 28 CA3), while black x's represent two groups of higher rate, putative inhibitory cells. B-C) Trajectory plots and ratemaps for all putative interneurons recorded on the final day of recording. B) Firing of all high rate (>10 Hz) cells recorded on the final day (circled cells in A). For each cell, the firing is shown in all four environments. On the top, the trajectory of the rat is plotted in gray with red dots showing the location of the rat for each spike, and on the bottom is the firing ratemap with the mean firing rate of the cell during that session shown above the ratemap. These cells did not have spatially selective firing and had properties typical of hippocampal interneurons, and were thus excluded from our analysis. C) Firing of all mid-rate/low burstiness cells, plotted the same as in B. These cells did not display spatially selective firing, were most often recorded in the hilus (3 in hilus, 1 in CA3, 1 in GCL) and resembled the firing of a hilar interneuron identified by juxtacellular labeling (Data S1D). These cells may represent a class of hilar interneurons and were also excluded from analysis.

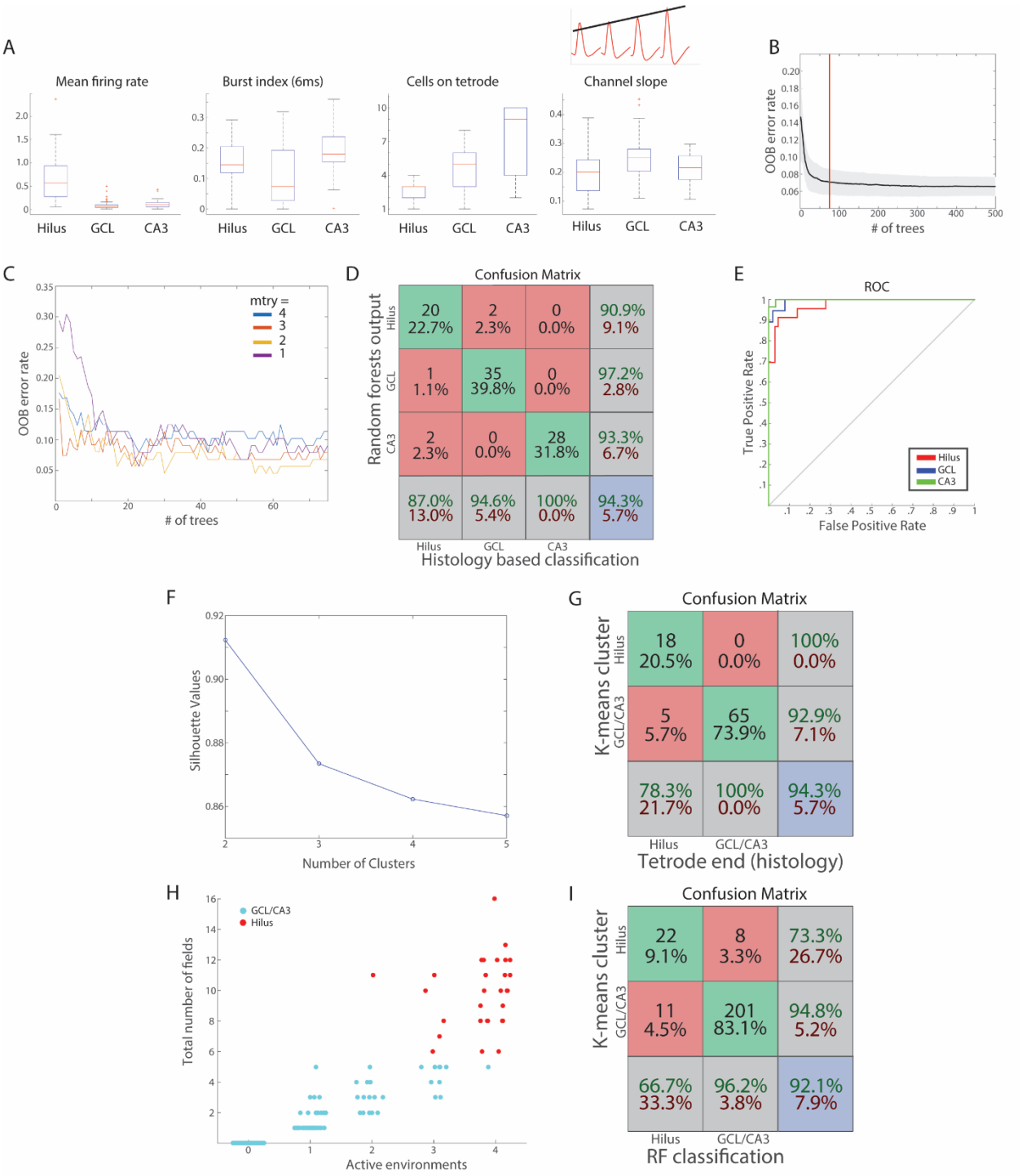

Figure S4. Random forests model, accuracy, and validation; related to Figure 4

A-E) Random forests classifier A) Boxplots of features used for training random forests classifier. Left to right, mean firing rate, burst index, number of well-isolated putative excitatory cells recorded on the same tetrode, and channel slope (Neunuebel and Knierim, 2012). Above the channel slope plot is a depiction of how this value was calculated. The peak amplitude of the

average waveform of each tetrode wire was sorted from smallest to largest and normalized to the peak amplitude of the largest wire. The slope of the best fit line through the four wire peaks (black line) is the channel slope. The only feature used for classification that is not shown is whether the tetrode was closer to CA3 or the GCL based on histological reconstruction. B) Out of bag error rate as the number of trees increases. 1000 random forests classifiers were created and the mean (black) ± 1 standard deviation (shaded) is shown. As the error rate is relatively stable after 75 trees (red line), we used 75 trees in our model. C) Out of bag error rate as m-try, or the number of randomly selected features used at each node while training individual trees, is increased. The model with m-try = 2 performs slightly better than others. D) Confusion matrix of OOB error. Y axis represents the output of the classifier on out of bag samples and the X axis represents the actual class labels, determined by histology. E) ROC curve for classification of GCL, hilus, and CA3. Probability was defined by the number of votes for the correct class divided by the number of combined votes for the other two classes. The large areas under the ROC curve for the GCL, hilus, and CA3 shows strong performance of the classifier in each binary discrimination. F-I) K–means clustering. The features used for clustering were number of active rooms and the total number of firing fields in all rooms. F) The silhouette value is a measure of how similar a point is to its own cluster compared to all other clusters, and higher silhouette values suggest the point is more accurately clustered. The average silhouette value is plotted as a function of the number of clusters, revealing the presence of two clusters in the 88 cells recorded on the final day. The two clusters in the final day recordings appear to represent 1) hilar cells and 2) combined GCL/CA3 cells. G) Confusion matrix showing accuracy of clustering of final day recordings compared to the histological classification. The accuracy of the clustering on these 88 cells was 94.3%. H) Scatter plot of the number of active environments and total number of fields for all 242 cells. Jitter was added to the x axis for better visualization. The color of each point represents the cluster to which that cell belongs. I) Confusion matrix for K–means clustering and the random forests model for classification of all 242 cells. The two models make the same classification for 92.1% of cells.

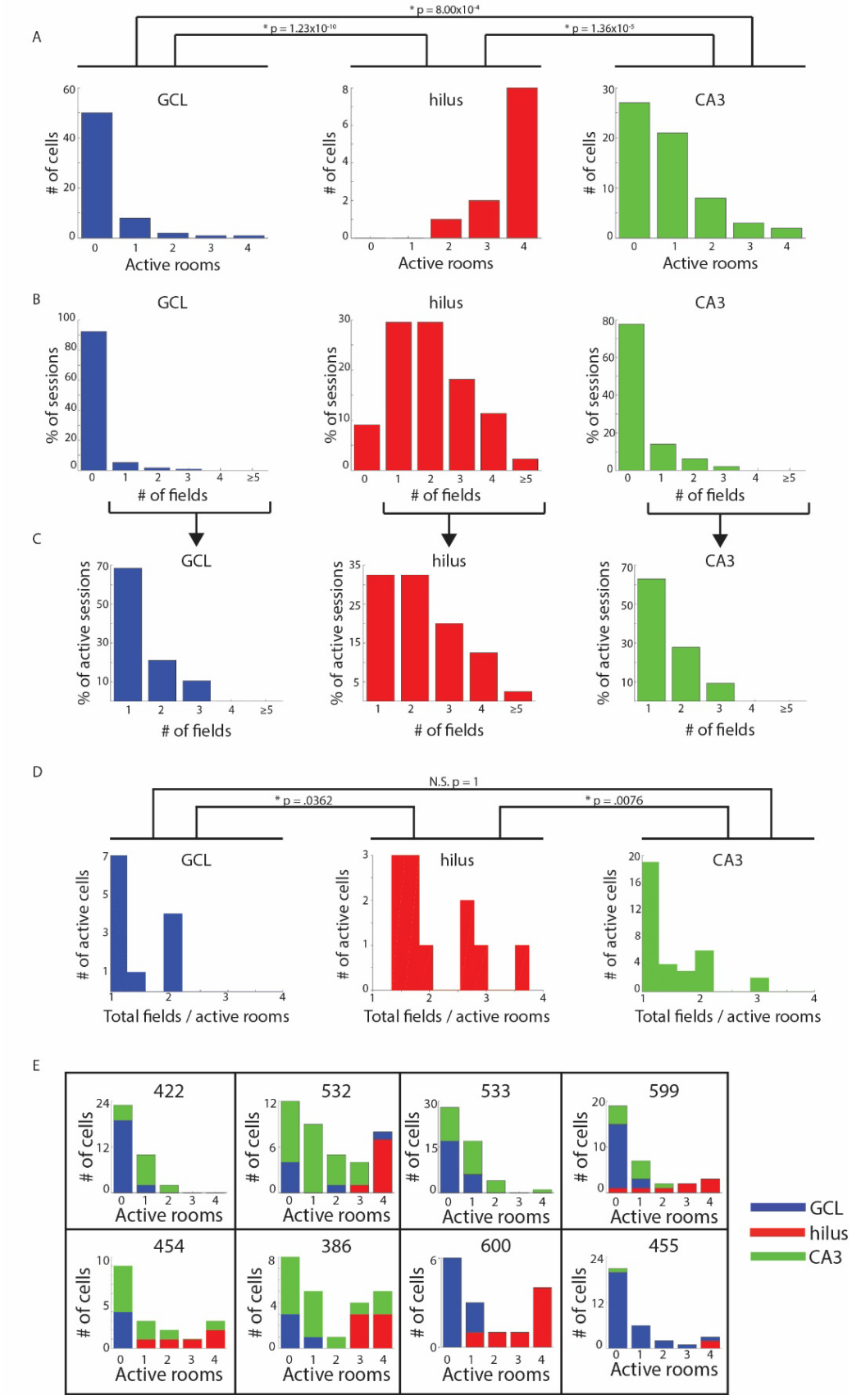
A
* p = 8.00x10-4
* p = 1.23x10-10
* p = 1.36x10-5
GCL
hilus
CA3
# of cells
Active rooms
B
% of sessions
# of fields
C
% of active sessions
D
N.S. p = 1
* p = .0362
* p = .0076
# of active cells
Total fields / active rooms
E
422
532
533
599
454
386
600
455
GCL
hilus
CA3

Figure S5. Consistent results from classified cells from tetrodes not used in initial (final day) analysis and across all animals; related to Figure 4

Since the full set of 242 cells includes some cells used in the initial analysis of cells recorded on the final day, we separately analyzed the 134 cells recorded on tetrodes not included in the initial analysis. The spatial firing of these 134 cells was no different from the results obtained from cells recorded on the final day (Figure 2) or all 242 cells (Figure 4). A) Number of active rooms; compare to Figure 2A, 4A. B) Number of fields in each recording session; compare to Figure 2B, 4B. C) Number of fields per session, excluding silent sessions; compare to Figure 4C. D) Histogram of number of fields per room (total number of fields divided by number of environments with fields); compare to Figure 4D. E) Number of active environments for all cells recorded in each of the 8 rats. Blue represents cells classified as GCL, red represents cells classified as hilus, and green represents cells classified as CA3. In all rats with cells active in all rooms, the majority of those cells were classified as hilus. In all animals, most cells silent in all four rooms or active in only one room were classified as GCL or CA3.

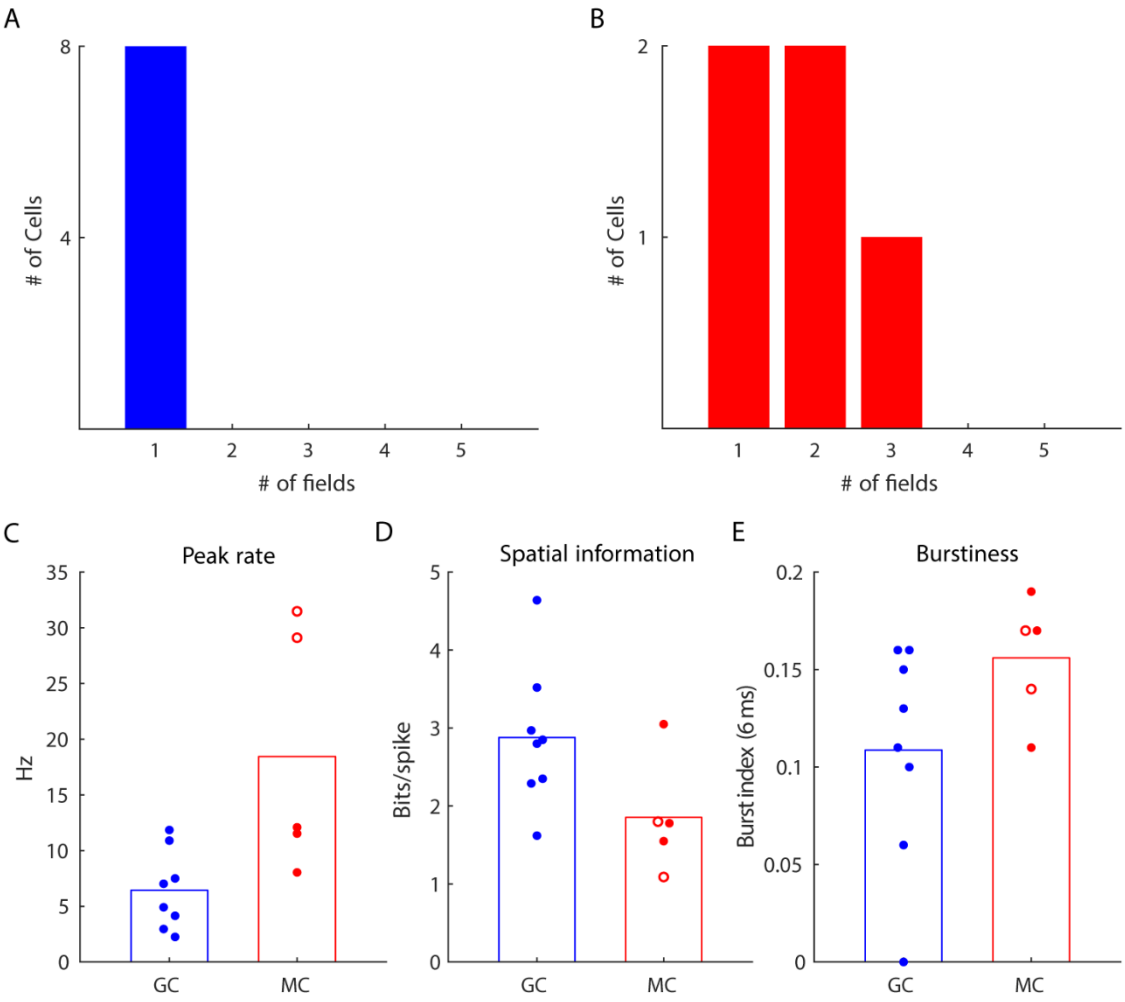

Figure S6. Statistics of juxtacellularly recorded granule cells and mossy cells; related to Figures 5-6

A-B) Number of fields of granule cells (blue) and mossy cells (red). Note the putative mossy cells in Data S1C are also included. One of these cells had two fields, and the other had a single (but multi-peaked) firing field. C-E) Peak rates (C), spatial information score (bits/spike), (D) and 6 ms burst indices (E) of granule cells (blue) and mossy cells (red). The open bars represent the mean value of each parameter and the solid dots represent each identified granule cell or mossy cell. The open red circles in (C-E) correspond to the putative mossy cells in Data S1C. Because of the low numbers, we present these data for illustrative purposes only; we did not attempt any statistical analyses.

Data S1. Spatial firing of all cells; related to Figures 3-6

A-G) All plots and rate maps of all juxtacellularly labeled hippocampal cells not illustrated in the main text. Convention is the same as Figures 5-6. A) Five granule cells. B) One putative interneuron in the GCL. C) Two putative mossy cells in the hilus. Arrows indicate the tracer deposits at the end of the glass electrodes (Duque and Zaborszky, 2006) in the hilus. One cell (bottom) was considered to have a single field using our field detection criteria, but the ratemap reveals multiple firing peaks, more similar to the multi-field firing of mossy cells than the clear single fields seen in identified granule cells. D) One hilar interneuron negative for GluR2/3. This cell did not show spatial selectivity and had low burstiness (6-ms burst index = 0.03). The mean firing rate of this cell was 4.43 Hz. E) Three CA3 cells. F) Six CA1 cells. G) One putative interneuron in CA1. H-J) Active cells from tetrode recordings, divided by random forests classification into hilus, GCL, and CA3. The spatial firing of all cells out of the 242 cells that were active in at least one environment is shown. H) 32 active cells classified as hilar recordings. Only one cell was silent in all four environments (3.03% of hilus cells) and is not shown. I) 25 active cells classified as GCL recordings; 87 cells that were silent in all environments (77.6% of GCL cells) are not shown. J) 59 active cells classified as CA3 recordings. 38 cells that were silent in all environments (39.2% of CA3 cells) are not shown. For all cells, the trajectory (gray) and spiking (red) is shown for all four foraging sessions. If significant spatial firing was detected in an environment, the rate map for that session was plotted below, with the peak firing rate of the cell between the two. On the left, the rat number (r) and tetrode number (tt) are listed for each cell.

Table S1: Statistical tests for tetrode recordings; related to Figures 2, 4, S5

Tests are shown for cells recorded on the final day of recording and on tetrodes located clearly in the GCL, hilus, or CA3 (related to Figure 2), for cells classified using the random forests classifier (related to Figure 4), and for the subset of cells classified using the random forests classifier but recorded on tetrodes that were not included in the initial analysis (related to Figure S5). These 134 cells came from tetrodes that either did not end clearly in the hilus, GCL, or CA3, and/or did not record cells on the final day of recording.

The values shown for the hilus, GCL, and CA3 represent the mean ± S.E.M, and n is the number of cells unless otherwise stated. The statistical tests used are listed for each comparison. For χ^2 tests the χ^2 statistic and p value for the comparison among all three groups are shown as well as χ^2 values and p values for the three pairwise χ^2 tests. For Kruskal-Wallis (KW) tests, the χ^2 statistic and p value are shown as well as the p values and z values for all pairwise Dunn's tests. All χ^2 and Dunn's test p values are corrected for multiple comparisons using Šidák's adjustment. Statistically significant results (adjusted p value < .05) are marked by asterisks, non-significant results are marked N.S. Spatial information scores for the classified cells are presented in bits/second as well as bits/spike for comparison with the results of Senzai and Buzsaki (in press).

Video S1. Firing of putative GC in sleep and wake, related to Figures 2, S2

The video has been sped up 4x. The activity of a putative granule cell can be heard. The rat is awake and can be seen grooming, moving around the dish and looking around the room during approximately the first half of the video. During this time very few spikes are heard. After ~1 minute, the rat rests his head on the edge of the dish as he falls asleep. After this point intermittent spikes can be heard much more frequently.